



Research Article

Palladium(0) Nanoparticles Immobilized onto Silica/Starch Composite: Sustainable Catalyst for Hydrogenations and Suzuki Coupling

Ravinderpal Kour Sodhi*, Satya Paul

Department of Chemistry, University of Jammu, Jammu-180 006, India

Received: 22nd February 2019; Revised: 27th May 2019; Accepted: 2nd June 2019;
Available online: 30th September 2019; Published regularly: December 2019

Abstract

The present paper aims to give insight into the art in the field of the synthesis, characterization and applications of Pd(0) nanoparticles immobilized onto silica/starch composite (SS-PdNPs) for hydrogenations and Suzuki coupling. Metal(0) nanoparticles immobilized onto silica/starch composite [SS-MNPs] were prepared from different metal acetylacetonate complexes [Co(acac)₂], [Cu(acac)₂], [Pd(acac)₂], [Ru(acac)₃], [Mn(acac)₃], [Co(acac)₃] by immobilizing onto silica/starch composite, followed by reduction with NaBH₄. Excellent yield of the products, reusability and the facile work-up makes SS-PdNPs a unique catalyst for the reduction of nitroarenes/carbonyl compounds, α,β unsaturated carbonyl compounds and Suzuki coupling under environmentally benign reaction conditions. All the catalysts were characterized by Fourier Transform Infra Red (FTIR), Atomic Absorption Spectroscopy (AAS) analyses, while the most active catalyst [SS-PdNPs] was further characterized by Scanning Electron Microscopy (SEM) and Transmission Electron Microscopy (TEM). Copyright © 2019 BCREC Group. All rights reserved

Keywords: Silica/starch composite; palladium(0) nanoparticles; hydrogenations; Suzuki coupling; heterogeneous catalysis

How to Cite: Sodhi, R.K., Paul, S. (2019). Palladium(0) Nanoparticles Immobilized onto Silica/Starch Composite: Sustainable Catalyst for Hydrogenations and Suzuki Coupling. *Bulletin of Chemical Reaction Engineering & Catalysis*, 14(3): 586-603 (doi:10.9767/bcrec.14.3.4395.586-603)

Permalink/DOI: <https://doi.org/10.9767/bcrec.14.3.4395.586-603>

1. Introduction

Bio-composites represent the new generation of nanocomposites, and comprises of the combination of biopolymers and an inorganic material [1-2]. The biopolymer-containing hybrid composite materials of silica have drawn attention owing to their promising properties and biocompatibility with living matter [3-7]. However, poor mechanical properties and high permeability to water are the two main disadvantages of biopolymers that recently nanotechnology helps to

solve. Polysaccharides being renewable, biodegradable and multifunctional are the attractive materials for silica bio-composite synthesis. Silica component in such hybrids is responsible for the properties like temperature and mechanical resistance, porosity, while the biopolymer offers extra functionality and framework to the hybrid matrices. Similar to conventional nanocomposites, which involve synthetic polymers, these bio-hybrid materials exhibit improved structural and functional properties of great interest for different applications. Mechanical properties of starch are influenced by many factors such as

* Corresponding Author.

E-mail: sodhiravinderpal@yahoo.com (R.K. Sodhi);

amylose to amylopectin ratio in starch that plays an important role in the mechanical properties of the films [8-9]. However, starch alone has some disadvantages, such as: hydrophilic nature and poor mechanical properties [10].

Composites containing functional metal NPs have attracted a great deal of attention, due to their unique optical, electrical, and catalytic properties [11]. They can be prepared by the mechanical mixing of a support with metal NPs, the *insitu* polymerization of a monomer in the presence of metal NPs, or the *insitu* reduction of metal salts or complexes. Recent advances in the design and preparation of supported metal nanoparticles confirmed that a numerous variety of metal nanoparticles can nowadays be synthesized through different preparation routes and supports to give tailored sizes, shapes and distributions, overcoming the main drawbacks of traditional synthetic methodologies. It is well known that the amount of metal, the size of the particles, the preparation method, and the support composition play crucial roles in the performance of heterogeneous catalysts. By employing transition metal nanoparticles of uniform size and shape, the reaction activities and product selectivities of many heterogeneous catalytic reactions could be greatly influenced [12-13]. With the growing interest in the heterogeneous catalysis, it is certain that organic/inorganic composites will still continue to be a fast moving topic for next several years.

It is well known that hydrogenation and Suzuki couplings catalyzed by Pd(0) nanoparticles are of significant importance in modern chemical transformations. The selective reduction of nitro compounds to amines is a synthetically important transformation leading to valuable starting materials and intermediates [14-15]. Recently, many novel reducing agents have been reported in literature [16-25]. However, the selective reduction of nitro group in the presence of other reducible functionalities in a molecule is a challenging task. In addition, reduction of aromatic nitro compounds often stops at an intermediate stage, leading to hydroxylamines, hydrazines, and azoarenes as side products [26]. The reduction of carbonyl compounds to alcohols is one of the most widely used and fundamental transformations in organic chemistry [27]. Transition metal catalyzed hydrogenations [28-29], biocatalytic and chemical reductions [30-39] have been utilized to accomplish the reduction of the carbonyl group. Chemoselective reduction of conjugated carbonyl compounds is a useful functional group transformation. Selective 1,4-reduction

of α,β -unsaturated carbonyl compounds has not been developed much and has always been a challenging problem in organic synthesis [40-42]. In case of chalcones having other reducible functional groups, the desired selectivity is hard to achieve. Some low-valent metal/Lewis acid reductive system [43-46], could selectively reduce the double bond of the α -enone system to the corresponding saturated analogue without affecting C=C bond present in the molecule, but none of them had been reported to be used in the conversion of chalcones to dihydrochalcones.

Suzuki cross-coupling reaction is an important method for carbon-carbon bond formation, which is a highly useful and versatile technique needed for the development of modern drug discovery, and in the synthesis of many natural products, polymers and other organic compounds. Traditional synthesis of biaryl derivatives [47] such as the Scholl reaction [48-49], the Gomberg-Bachmann reaction [50-51], or Ullmann-type couplings [52-53] require rather harsh conditions and often suffer from low yields in case of unsymmetrically substituted biaryls, while recent strategies including processes that involve directed ortho-metalation, are limited to a narrow range of substrates [54]. Catalytic cross-coupling reaction of organotin [55-58], zinc [59], copper [60], boron [61], or magnesium compounds [62-64] constitute the most generally applicable strategy for the synthesis of biaryls. Over the past decades, it has continuously been improved and reached an impressive level of performance [65-68].

Due to our continued interest in the development of heterogeneous catalysis [69-73], herein we report the synthesis of different metal(0) nanoparticles immobilized onto silica/starch composite (MNPs) and their catalytic activities have been evaluated for the selective reduction of nitroarenes/carbonyl compounds, α,β -unsaturated carbonyl compounds and "Suzuki coupling" with a view to select the most effective recyclable and stable heterogeneous catalyst.

2. Materials and Methods

2.1 Materials and Characterizations

The chemicals used were either prepared in our laboratories or purchased from Aldrich Chemical Company or Merck. The ^1H and ^{13}C NMR data were recorded in CDCl_3 or $\text{DMSO}-d_6$ on Bruker Avance III 400 MHz. The FTIR spectra were recorded on Perkin-Elmer FTIR spectrophotometer and mass spectral data

were recorded on Bruker Esquires 3000 (ESI). SEM images were recorded using FEG SEM JSM-7600F Scanning Electron Microscope and Transmission Electron Micrographs (TEM) on H7500 Hitachi. The amount of metal in catalysts was determined by AAS analysis and thermal analysis was carried out on Linsesis STA PT-1000 make thermal analyzer.

2.2 General Procedure for the Synthesis of Metal(0) Nanoparticles Immobilized onto Silica/Starch Composite [SS-MNPs]

A mixture of silica/starch composite [59b] (3 g) and $M(\text{acac})_n$ [0.5 mmol, 0.12 g $\text{Co}(\text{acac})_2$, 0.13 g $\text{Cu}(\text{acac})_2$, 0.15 g $\text{Pd}(\text{acac})_2$, 0.19 g $\text{Ru}(\text{acac})_3$, 0.17 g $\text{Co}(\text{acac})_3$ and 0.12 g $\text{Mn}(\text{acac})_3$] in absolute ethanol (30 mL) was stirred at room temperature for 3 h followed by slow addition of NaBH_4 (0.5 g, 13 mmol). The reaction mixture was stirred for another 12 h

Table 1. AAS analysis^a (metal / g.cat) of SS-MNPs

Entry	Catalyst	AAS analysis (Metal wt%)
1	SS-CoNPs	1.1
2	SS-CuNPs	1.2
3	SS-PdNPs	1.8
4	SS-MnNPs	0.9
5	SS-RuNPs	1.9

^a AAS analysis was carried on GBC Avanta-M Atomic Absorption Spectrometer.

Table 2. Comparison of catalytic activities of different metal(0) nanoparticles immobilized onto silica/starch composite for the reduction of nitro and carbonyl groups/selective reduction of C=C double bond/Suzuki coupling

Entry	Catalyst	Reduction of nitro/carbonyl group ^a				Selective reduction of C=C double bond ^b		Suzuki coupling ^c	
		Nitroarene		Aldehyde		Time (h)	Yield ^e (%)	Time (h)	Yield ^e (%)
		Time (h)	Yield ^d (%)	Time (h)	Yield ^d (%)				
1	SS-CoNPs	1	70	2	70	1	65	-	-
2	SS-CuNPs	1	60	2	65	1	50	-	-
3	SS-PdNPs	0.5	92	1.5	90	1	90	0.25	94
4	SS-MnNPs	1	50	2	60	1	60	-	-
5	SS-RuNPs	1	80	2	60	1	50	-	-

^aReaction conditions: nitrobenzene or benzaldehyde (1 mmol), SS-MNPs (4 mol% M, M= Cu, Ru, Pd, Co, Mn) using molecular H_2 in water (5 mL) for nitrobenzene, and water/ethanol (3:1) for benzaldehyde at room temperature.

^bReaction conditions: (*E*)-1-(4-chlorophenyl)-3-phenylprop-2-en-1-one (0.242 g, 1 mmol), SS-MNPs (4 mol % M, M= Cu, Ru, Pd, Co, Mn) using molecular H_2 in CH_3CN (5 mL) at room temperature.

^cReaction conditions: 4-bromoacetophenone (0.199 g, 1 mmol), benzeneboronic acid (0.145 g, 1.2 mmol), K_2CO_3 (0.207 g, 1.5 mmol), TBAB (0.154 g, 1 mmol) and catalyst (4 mol% M, M= Cu, Ru, Pd, Co, Mn) using water (5 mL) as solvent at 100 °C.

^dColumn chromatography yield.

^eIsolated yields.

and then filtered, washed with ethanol (3×15 mL) followed by diethyl ether (2×15 mL). Finally the catalysts were vacuum dried at 100 °C for 5 h.

2.3 General Procedure for the SS-PdNPs Catalyzed Hydrogenation of Nitroarenes, Aldehydes and Ketones at Room Temperature

To a mixture of nitroarene or aldehyde or ketone (1 mmol) and SS-PdNPs (0.2 g, 1.8 wt% Pd) in a round bottom flask (25 mL), water (5 mL for nitroarenes) or water/ethanol (3:1, 5 mL for aldehydes or ketones) was added and the reaction mixture was stirred at room temperature using balloon filled hydrogen for an appropriate time (Table 2). After completion, the reaction mixture was diluted with hot ethyl acetate and filtered. The residue was washed with hot ethyl acetate (3×10 mL) followed by double distilled water (3×10 mL). The organic layer was washed with water and dried over anhydrous Na_2SO_4 . Finally, the product was obtained after removal of the solvent under reduced pressure followed by crystallization with EtOAc: pet ether/column chromatography. The catalyst was dried at 100 °C for 2 h and could be used in subsequent reactions.

2.4 General Procedure for the SS-PdNPs Catalyzed Selective Reduction of C=C Double Bond in α,β -unsaturated Ketones

To a mixture of α,β -unsaturated ketone (1 mmol) and SS-PdNPs (0.2 g, 1.8 wt% Pd) in a round bottom flask (25 mL), acetonitrile (5 mL)

was added and the reaction mixture was stirred at room temperature using balloon filled hydrogen for an appropriate time. The product was obtained after the similar work-up as given in Section 2.3.

2.5 General Procedure for the SS-PdNPs Catalyzed Suzuki Coupling in Aqueous Medium

To a mixture of aryl halide (1 mmol), aryl/heteroaryl boronic acid (1.2 mmol), TBAB (1 mmol), K_2CO_3 (1.5 mmol) and SS-PdNPs (0.2 g, 1.8 wt% Pd) in a round bottom flask (25 mL), water (5 mL) was added, and the reaction mixture was stirred at 100 °C for an appropriate time (monitored by TLC). The product was obtained after the similar work-up as given in Section 2.3. The structures of the products were confirmed by 1H , ^{13}C NMR, mass spectral data and comparison with authentic samples available commercially or prepared according to the literature methods.

3. Results and Discussion

3.1 Characterization of Metal(0) Nanoparticles Immobilized onto Silica/starch Composite [SS-MNPs]

The textural properties of silica/biomaterials present a unique chemical environment in which nano-particles can be synthesized. Due to the presence of a silica backbone, the mechanical stability of the silica/starch composite is quite high compared to that of pure organic polymers or other microporous organic polymers. So, we have chosen silica/starch material for the preparation of supported metal nanoparticles. Metal(0) nanoparticles immobilized onto silica/starch composite [SS-MNPs] were prepared from different metal acetylacetonate complexes [$Co(acac)_2$, $Cu(acac)_2$, $Pd(acac)_2$, $Ru(acac)_3$, $Mn(acac)_3$, $Co(acac)_3$] by immobilizing onto silica/starch composite, followed by reduction with $NaBH_4$ (Scheme 1).

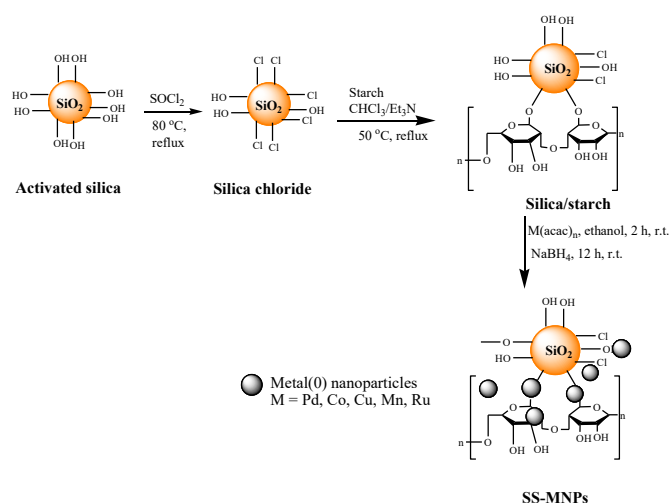
All the five SS-MNPs were characterized by FTIR and AAS analyses. In addition to this, the most active catalyst, SS-PdNPs was further characterized by Thermogravimetric analysis (TGA), Scanning Electron Microscopy (SEM) and Transmission Electron Microscopy (TEM). The FTIR spectrum of Pd(0) nanoparticles supported onto silica/starch substrate (SS-PdNPs, Figure 1) showed three bands at around 1642, 802, and 576 cm^{-1} , which are presumably due to $\nu_{as}(Si-O-Si)$ and $\nu_s(Si-O-Si)$ and bending modes of Si-O-Si, respectively. The weak band at 2089 cm^{-1} is due to the stretching vibration of C-H and C-C bonds. Also, the band at 1418 cm^{-1} is

associated with the stretching vibration of the C-O bond.

The stability of the catalysts was determined by Thermo-gravimetric analysis (TGA). The TGA was recorded by heating the sample at the rate of 10 °C.min $^{-1}$. The TGA curve of SS-PdNPs showed an initial weight loss up to 100 °C which was attributed to the loss of residual solvent and water trapped onto the surface of silica. The second weight loss above 251 °C (and continuing to 404 °C) is related to the decomposition of starch from the silica substrate (Figure 2). The amount of the metal supported onto silica/starch composite was determined by Atomic Absorption Spectroscopy (AAS). SS-PdNPs contained 1.8 wt% of palladium. The AAS of all the five catalysts is presented in Table 1.

The surface morphology of supported silica-starch palladium(0) nanoparticles was studied using a Scanning Electron Microscopy (SEM). The SEM images showed that the catalyst has a porous structure with particle size in the range of 15-18 nm (Figure 3). The TEM images provided a direct observation of the morphology and distribution of palladium nanoparticles onto the surface of silica/starch composite (Figure 4). The regular arrangement of the pores can be clearly observed. The Pd(0) nanoparticles are uniformly distributed with an average diameter of about 2 nm. No bulk aggregation of the metal occurred indicating that palladium is dispersed evenly onto the surface the support material.

The histogram revealing the size distributions of Pd(0) nanoparticles is shown in Figure 5 which is proposed according to the



Scheme 1. Synthesis of metal(0) nanoparticles immobilized onto silica/starch composite [SS-MNPs].

data obtained from the TEM image. The average size of the Pd nanoparticles was found to be 3.5 nm.

3.2 Catalytic Testing for the Hydrogenation of Nitroarenes, Aldehydes, and Ketones at Room Temperature under Aqueous Medium

In order to identify the best catalytic system for the reduction of nitro and carbonyl groups, various metal nanoparticles immobilized onto silica/starch composite were synthesized (SS-MNPs, M = Pd, Co, Cu, Mn, Ru) and their catalytic activities were evaluated for the reduction selecting nitrobenzene and benzaldehyde as the test substrates using molecular H₂ at room temperature. The results are presented in Table 2. Among the different catalysts

screened, palladium(0) nanoparticles immobilized onto silica/starch composite [SS-PdNPs] provided the best results.

The most widely used methods for the reduction of nitro groups make use of hydrazine hydrate or molecular hydrogen [40]. In the recent years, due to stringent environmental legislation, cleaner and safer procedures using molecular hydrogen became more attractive to the chemists. This method produces only water as a by-product and therefore no toxic and hazardous wastes are produced. Thus, a lot of efforts have been devoted to the development of catalytic hydrogenation of the organic nitro compounds using molecular hydrogen as the reductant. Screening of various solvent systems using SS-PdNPs catalyst showed that water and water/ethanol mixture is the most suit-

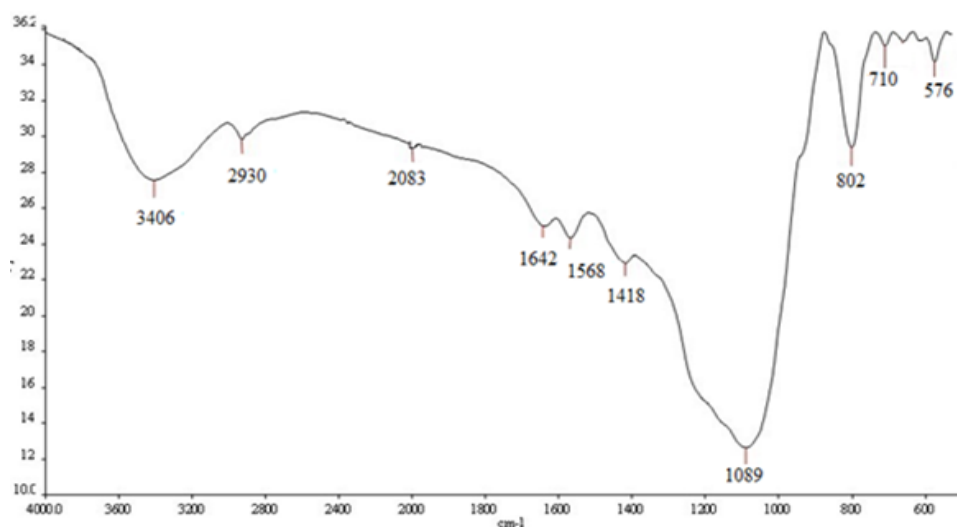


Figure 1. FTIR spectra of SS-PdNPs

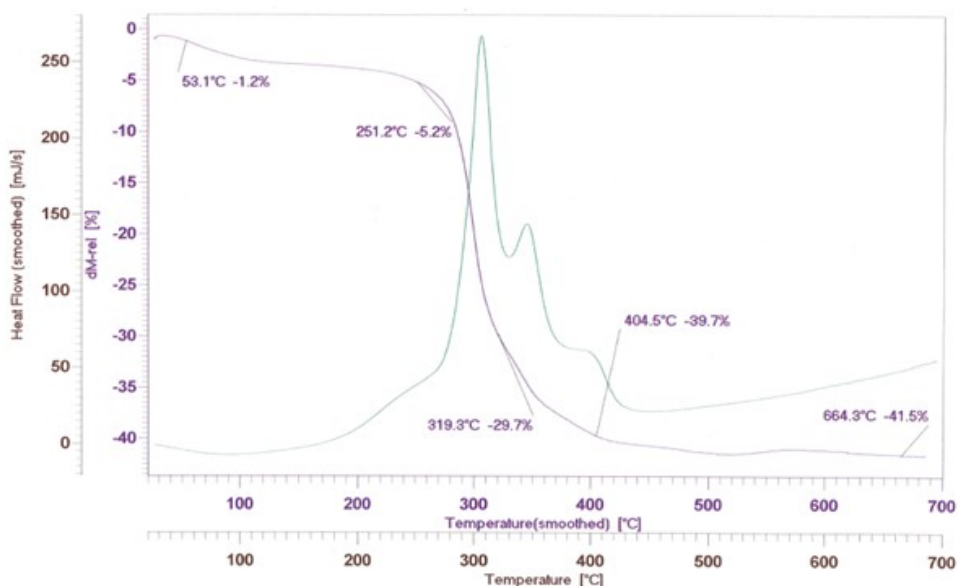


Figure 2. TGA of SS-PdNPs

able solvent for reduction of nitro- and carbonyl groups respectively. The reaction worked selectively and efficiently with a wide range of nitro substituted aromatic compounds under hydrogen atmosphere at room temperature (Scheme 2, Table 3).

Even in the presence of electron-donating groups (Table 3, entries 2a, 2b, 2d), the reaction proceeded efficiently to afford the products in quantitative yields. It is worthy to note that the azoxy, azo and hydrazo compounds as the usual side products of reduction of nitroarenes were not observed in this method. To widen the scope of the catalytic system, various aldehydes (entries 3a-3e) and ketones (entries 3f-3h) were subjected to reduction to their corresponding alcohols (Scheme 2). However, the results were unsatisfactory. The reduction of carbonyl compounds, which are poorly soluble in water, needed long reaction time for their completion, while water/ethanol mixture (3:1) improved the

solubility and accelerated the reaction. Thus, for the reduction of carbonyl compounds, water/ethanol (3:1) was used as solvent. Aromatic aldehydes bearing electron-donating groups or electron-withdrawing groups were reduced to alcohols in excellent yields at room temperature. Reduction of ketones also underwent smoothly and gave corresponding secondary alcohols in excellent yields.

3.3 Catalytic Testing for the Selective Reduction of Carbon-carbon Double Bond in α,β -unsaturated Ketones at Room Temperature

In order to optimize the reaction conditions, (*E*)-3-(4-chlorophenyl)-1-phenylprop-2-en-1-one was selected as the test substrate and the reaction was carried out under different set of conditions with respect to different solvents, temperatures and supported metal catalysts. In order to select the most efficient catalyst, the reaction with test substrate was carried out with

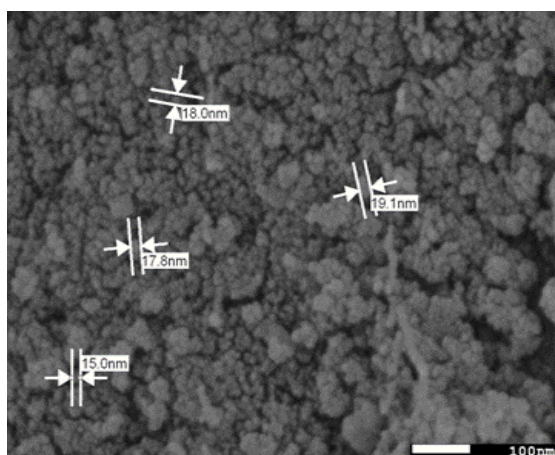


Figure 3. SEM image of SS-PdNPs

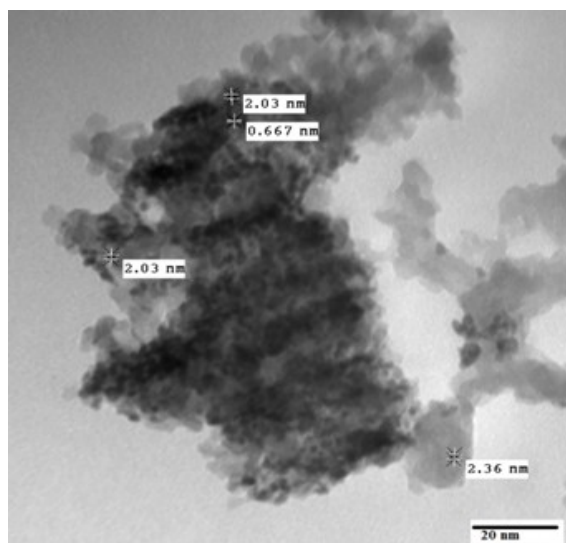
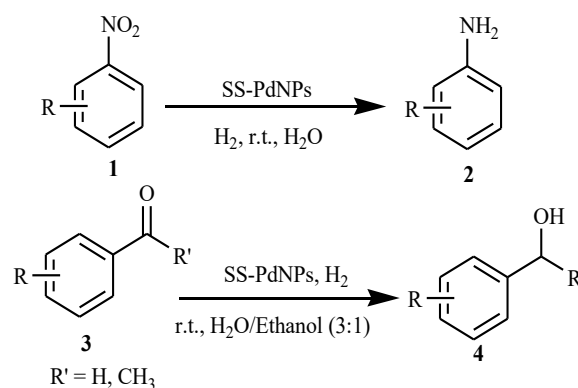


Figure 4. TEM image of SS-PdNPs



Scheme 2. SS-PdNPs catalyzed reduction of nitroarenes, aldehydes and ketones.

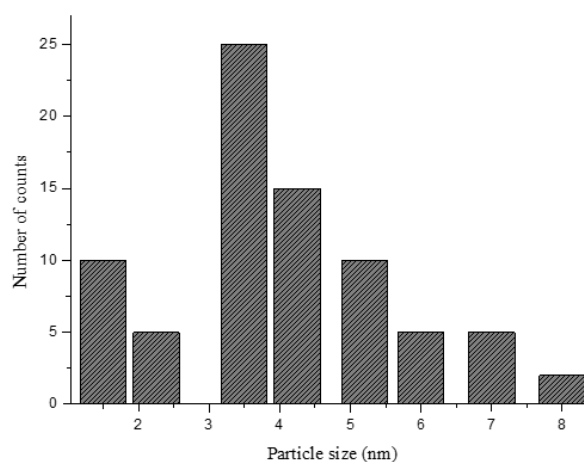
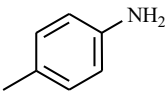
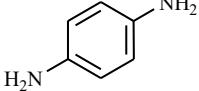
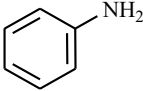
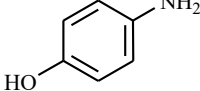
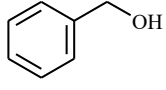
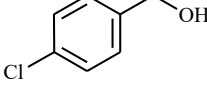
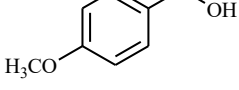
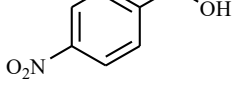
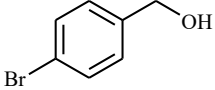
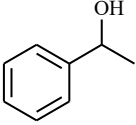
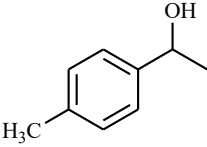
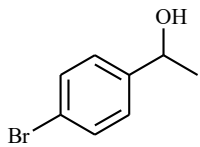


Figure 5. A histogram representing the size distribution of Pd nanoparticles on the silica/starch substrate

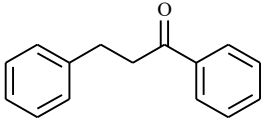
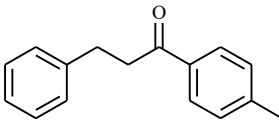
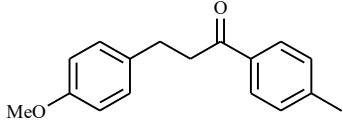
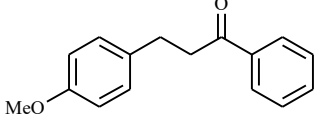
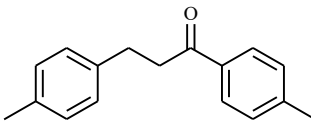
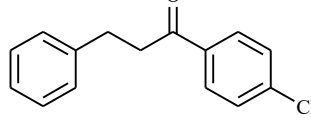
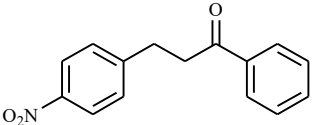
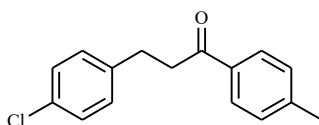
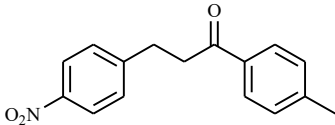
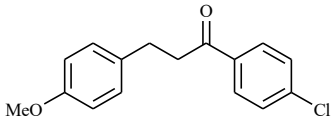
Table 3. SS-PdNPs catalyzed reduction of nitroarenes, aldehydes and ketones^{a,b}

 2a: 0.5h, 93%	 2b: 1h, 90%	 2c: 2h, 87%	 2d: 4h, 85%
 3a: 1.5h, 90%	 3b: 2h, 92%	 3c: 5h, 83%	 3d: 2h, 87%
 3e: 1h, 85%	 3f: 1.5h, 87%	 3g: 3h, 80%	 3h: 1.5h, 85%

^a Reaction conditions: nitroarene or aldehyde or ketone (1 mmol), SS-PdNPs (0.2 g, 1.8 wt% Pd) at room temperature using molecular H₂ in water (5 mL) for nitroarenes and water/ethanol (3:1, 5 mL) for aldehydes and ketones.

^b Isolated yields/Column chromatography yield.

Table 4. SS-PdNPs catalyzed selective reduction of C=C double bond in α,β unsaturated ketone^{a,b}

 6a: 1.5h, 85%	 6b: 1h, 85%	 6c: 2.75h, 87%
 6d: 1.5h, 85%	 6e: 2h, 78%	 6f: 1h, 90%
 6g: 1.25h, 83%	 6h: 2h, 87%	 6i: 2.5h, 88%
 6j: 1.5h, 80%		

^aReaction conditions: α,β -unsaturated ketone (1 mmol), molecular H₂ (ballon), SS-PdNPs (0.2 g, 1.8 wt% Pd), acetonitrile (5 mL) at room temperature.

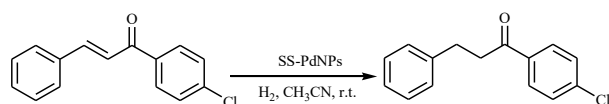
^bIsolated yield.

different SS-MNPs [where M = Pd, Co, Cu, Ru, Mn]. After carrying out series of reactions, it was found that SS-PdNPs catalyzes the reaction selectively with excellent yield (Table 2). Further, the reaction with test substrate was also carried out using different solvents such as toluene, acetonitrile, ethanol and water. Among these, acetonitrile was found to be best solvent at room temperature, since with toluene and water, conversion was poor and in case of ethanol moderate results were obtained. To test the generality and versatility of the developed procedure, α,β -unsaturated ketones substituted with different groups were subjected to selective reduction under the selected conditions and excellent results were obtained (Scheme 3, Table 4).

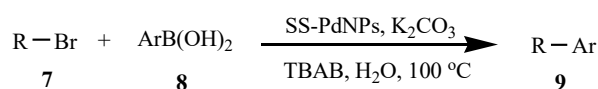
3.4 Catalytic Testing for the Suzuki Coupling in Water

In order to select the optimum reaction conditions for the Suzuki coupling, 4-bromoacetophenone and benzene boronic acid were selected as the test substrates and the reaction was carried out under different set of conditions with respect to different supported palladium catalysts, solvents and temperatures. To find out the most efficient catalyst for the desired coupling, reaction was carried out in the presence of different supported palladium catalysts. The results are shown in Table 5. It was found that SS-PdNPs was superior to the other two catalysts in terms of selectivity, reaction time and yield (Table 2, Table 5).

In the recent years, there has been considerable attention dedicated to the development of organic reactions in water [27]. So, we attempted the reaction between 4-bromoacetophenone (1 mmol) and benzene boronic acid (1.2 mmol), K_2CO_3 (1.5 mmol) as base in the presence of SS-PdNPs using water as solvent and found that reaction was successful but complete con-



Scheme 3. SS-PdNPs catalyzed selective reduction of α,β -unsaturated ketones.



Scheme 4. SS-PdNPs catalyzed synthesis of biaryls/polyaryls *via* Suzuki coupling.

version did not take place. This may be due to the poor solubility of substrates in water. In order to further improve the reaction conditions, TBAB (1 mmol) was added and found that complete conversion of 4-bromoacetophenone took place with quantitative yield in 15 min. Thus, TBAB enhances the rate of reaction by transferring haloarene to the aqueous phase and hence reacting with phenyl boronic acid faster. K_2CO_3 was selected as the base, since it is inexpensive and easily available. The generality of the developed protocol was studied by choosing different aryl halides substituted with both electron-donating and electron-withdrawing groups, and good to excellent results were obtained (Scheme 4, Table 6). Heteroarylboronic acids are generally considered as the poor substrates for the Suzuki coupling, our methodology making use of SS-PdNPs found to be highly efficient for the Suzuki coupling of *S*-heteroarylboronic acids in water (entry 10, Table 6).

3.5 Effect of Catalyst Loading on the Reduction of Nitro/Carbonyl Groups, Selective Reduction of C=C Double Bond and Suzuki Coupling

Finally, to investigate the effect of catalyst on the reaction, different amounts of catalysts were tested. The test reactions were carried out using different amounts of the catalyst i.e. 0.05 g, 0.10 g, 0.15 g, 0.2 g, and 0.25 g. The results showed that the addition and increasing the concentration of catalyst, the rate of reaction was enhanced (Figure 6).

This may be due to the availability of large number of active sites on the surface of catalyst which increases with the amount of the

Table 5. Comparison of SS-PdNPs with other supported catalysts for Suzuki coupling^a

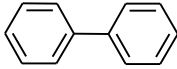
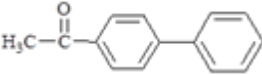
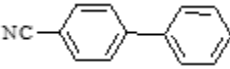
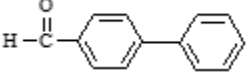
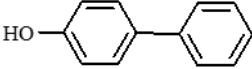
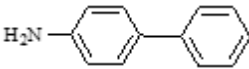
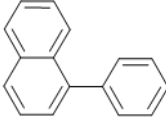

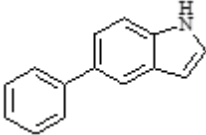
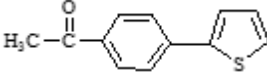
Entry	Catalyst ^b	Time (min)	Yield (%) ^c
1	ASS-Pd(acac) ₂ [59 ^b]	15	60
2	SiO ₂ -Pd(acac) ₂ [59 ^c]	15	70
3	SS-PdNPs	15	90

^aReaction conditions: 4-bromoacetophenone (0.199 g, 1 mmol), benzeneboronic acid (0.145 g, 1.2 mmol), K_2CO_3 (0.207 g, 1.5 mmol), TBAB (0.154 g, 1 mmol) and catalyst (1.8 wt% Pd) using water (5 mL) as solvent at 100 °C.

^bCatalyst: amine functionalized silica/starch-Pd(acac)₂ [ASS-Pd(acac)₂]; silica functionalized-Pd(acac)₂ [SiO₂-Pd(acac)₂]; silica/starch palladium(0) nanoparticles [SS-PdNPs].

^cIsolated yields.

Table 6. SS-PdNPs catalysed Suzuki coupling under aqueous medium at 100 °C^{a,b}

			
9a: 0.25h, 90%	9b: 0.5h, 90%	9c: 0.25h, 89%	9d: 0.5h, 90%
			
9e: 1.5h, 85%	9f: 1h, 85%	9g: 0.75h, 80%	9h: 1h, 75%
			
	9i: 2h, 70%	9j: 0.75h, 80%	

^aReaction conditions: aryl halide (1 mmol), benzenboronic acid/2-thiophene boronic acid (1.2 mmol), K₂CO₃ (1.5 mmol), TBAB (1 mmol), SS-PdNPs (0.2 g, 1.8 wt% Pd) and water (5 mL) at 100 °C .

^bIsolated yields.

Table 7. Comparison of activity of SS-PdNPs with different catalysts/precursors

Entry	Catalyst	Reduction of nitro/carbonyl group ^a				Selective reduction of C=C double bond ^a		Suzuki coupling ^a	
		Aniline		Alcohol		Time (h)	Yield ^b (%)	Time (h)	Yield ^b (%)
		Time (h)	Yield ^b (%)	Time (h)	Yield ^b (%)				
1	No catalyst	3	5	3	traces	2	traces	1	NR ^d
2	Silica	3	15	3	5 ^c	2	5 ^c	1	5 ^c
3	Starch	3	15	3	5 ^c	2	5 ^c	1	5 ^c
4	Silica/starch composite	3	20	3	10	2	15	1	10 ^c
5	SS-PdNPs	0.5	93	1.5	90	1	90	0.25	90
6	SiO ₂ -Pd(acac) ₂	0.5	75	1.5	70	1	75	0.25	70
7	ASS-Pd(acac) ₂	0.5	70	1.5	65	1	70	0.25	60

^aReaction conditions: Reduction of nitro/carbonyl group- nitrobenzene or benzaldehyde (0.123 g or 0.106 g, 1 mmol), H₂, catalyst (0.2 g for entries 2-4; and 4 mol% Pd for entries 5-7) at room temperature in water (5 mL) for nitrobenzene and water/ethanol (3:1, 5 mL) for benzaldehyde. Selective reduction of C=C double bond; (*E*)-1-(4-chlorophenyl)-3-phenylprop-2-en-1-one (0.242 g, 1 mmol), H₂, catalyst (0.2 g for entries 2-4; and 0.2 g, 4 mol% Pd for entry 5-7) at room temperature in CH₃CN (5 mL). Suzuki coupling; 4-bromoacetophenone (0.199 g, 1 mmol), benzenboronic acid (0.145 g, 1.2 mmol), K₂CO₃ (0.207 g, 1.5 mmol), TBAB (0.154 g, 1 mmol) and catalyst (0.2 g for entries 2-4; and 4 mol% Pd for entries 5-7) using water (5 mL) as solvent at 100 °C.

^bIsolated yield.

^cColumn chromatography yield.

^dNo reaction.

catalyst. Thus, 0.2 g (1.8 wt%) has been taken as an optimal catalyst concentration for the studied reaction.

In order to find out the role of SS-PdNPs as the heterogeneous catalyst, the reduction (using nitrobenzene and benzaldehyde as test substrate), selective reduction of selective reduction of C=C bond in α,β -unsaturated ketones (using (*E*)-1-(4-chlorophenyl)-3-phenylprop-2-en-1-one as test substrate) and Suzuki coupling (using 4-bromoacetophenone and benzenboronic acid as test substrates) was carried out in the presence of silica, starch, silica/starch composite, SS-PdNPs and without using catalyst. Out the different catalysts, SS-PdNPs catalyzes the reaction efficiently in terms of selectivity, reaction time and yield. The results are summarized in Table 7.

3.6 Heterogeneity and Recyclability

To rule out the contribution of homogeneous catalysis, the reaction in case of entry 2c, (Table 3) was carried out until the conversion was 50% (0.25 h) and at that point the solid was filtered off at the reaction temperature. The liquid phase was then transferred to another flask and again allowed to react, but no

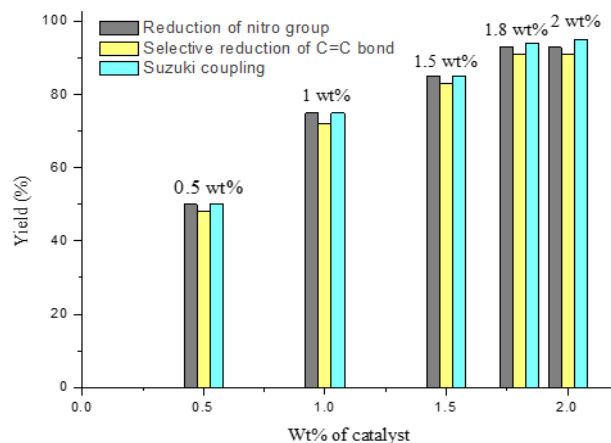


Figure 6. Effect of catalyst loading. Reaction conditions: ^anitrobenzene (1 mmol), SS-PdNPs (different loadings), molecular H₂ in water (5 mL) at room temperature (reduction of nitrobenzene); ^b(*E*)-1-(4-chlorophenyl)-3-phenylprop-2-en-1-one (0.242 g, 1 mmol), SS-PdNPs (different loadings), molecular H₂ in CH₃CN (5 mL) at room temperature (selective reduction of C=C); ^cReaction conditions: 4-bromoacetophenone (0.199 g, 1 mmol), benzenboronic acid (0.145 g, 1.2 mmol), K₂CO₃ (0.207 g, 1.5 mmol), TBAB (0.154 g, 1mmol) and SS-PdNPs (different loadings) using water (5 mL) as solvent at 100 °C (Suzuki coupling).

further significant conversion was observed. This indicates that no active species was present in the supernatant (no palladium was detected in the supernatant by AAS analysis). After evaluating the reaction results, the catalyst was collected, washed with solvents and then used again in the next reaction. The catalytic activity was maintained with high selectivity in all the reaction runs, which indicates an excellent recyclability (Table 8).

In order to examine the shape and morphology of the catalyst after five reaction runs, SEM and TEM measurements were carried out, and it seemed that the catalyst has not suffered to serious damage during the reactions. The average diameter of the SS-PdNPs was estimated to be somewhat similar to the fresh catalyst. However, irrespective of the cycle, the catalyst was invariably active. The amount of loaded Pd on the surface is 1.75 wt% after five successive runs, which indicates no leaching during the repeated runs.

4. Conclusions

In conclusion, we found that palladium(0) nanoparticles could be easily immobilized onto silica/starch surface, and which act as highly active and reusable catalyst for promoting hydrogenations and Suzuki couplings to produce the corresponding products in excellent yields with high chemo-selectivity and acceptable reaction times. Such designer materials have a significant impact in many areas including increasing applications in industrial catalytic processes. However, the preparation of these supported metal nanoparticles should be promoted in a more sustainable way, thus reducing waste generation and the use of toxic compounds with improved manufacturing safety as well as decreasing the production costs.

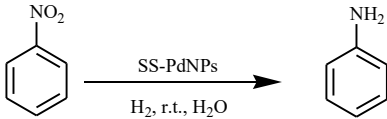
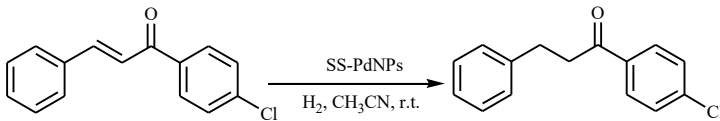
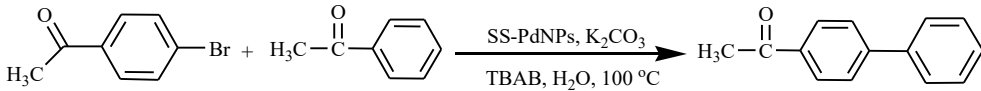
Acknowledgment

We thank the Head, SAIF, Punjab University Chandigarh for FT-IR and SEM; and Head, SAIF, IIT Bombay for TEM studies. We gratefully acknowledge Department of Science and Technology, Government of India for NMR spectrometer (Bruker Avance III, 400 MHz) under PURSE program to the Department of Chemistry, University of Jammu. We also thank UGC, New Delhi for financial support (SAP, DRS I and Major research project, F-41-281/2012 (SR).

References

- [1] Siracusa, V., Rocculi, P., Romani, S., Rosa, M.D. (2008). Biodegradable polymers for food-packaging: a review. *Trends in Food Science and Technology*, 19: 634-643.
- [2] Karim, A.A., Tie, A.P.L., Manan, D.M.A., Zaidul, I.S.M. (2008). Starch from the Sago (*Metroxylon sago*) Palm Tree-Properties, Prospects, and Challenges as a New Industrial Source for Food and Other Uses. *Comprehensive Reviews in Food Science and Food Safety*, 7: 215–228.
- [3] Gutowska, A., Jeong, B., Jasionowski, M. (2001). Injectable gels for tissue engineering. *Anat. Rec.*, 263: 342-349.
- [4] Livage, J., Coradin, T., Roux, C. (2001). Encapsulation of biomolecules in silica gel. *J. Phys. Condens. Matter*, 13: 673-691.
- [5] Ren, L., Tsuru, K., Hayahawa, S., Osaka, A. (2002). A Novel approach to fabricate porous gelatin-siloxane hybrids for bone tissue engineering. *Biomaterials*, 23: 4765-4773.
- [6] Sakai, S., Ono, T., Ijima, H., Kawakami, K. (2002). In vitro and in vivo evaluation of alginate/sol-gel synthesized aminopropyl silicate/alginate membrane for bioartificial pancreas. *Biomaterials*, 23: 4177-4183.
- [7] Schuleit, M., Luisi, P.L. (2001). Enzyme immobilization in silica-hardened organogels. *Biotechnol. Bioeng.*, 72: 249-253.
- [8] Alebooyeh, R., Nafchi, A.M., Jokar, M. (2012). The Effects of ZnO nanorodson the Characteristics of Sago Starch Biodegradable Films. *J. Chem. Health Risks*, 2: 13-16.
- [9] Nafchi, A.M., Moradpour, M., Saeidi, M., Alias, A.K. (2013). Thermoplastic starches: Properties, challenges, and prospects. *Starch-Srarke*, 65: 61-72.
- [10] Li, J.H., Hong, R.Y., Li, M.Y., Li, H.Z., Zheng, Y.J. (2009). Effects of ZnO nanoparticles on the mechanical and antibacterial properties of polyurethane coatings. *Prog. Org. Coat.*, 64: 504-509.
- [11] Laun, J., Wang, S., Hu, Z., Zhang, L. (2012). Synthesis Techniques, Properties and Applications of Polymer Nanocomposites. *Curr. Org. Synth.*, 9: 114-136.
- [12] Reddy, J.K., Motokura, K., Koyama, T., Miyaji, A., Baba, T. (2012). Effect of morphology and particle size of ZSM-5 on catalytic

Table 8. Recyclability data for hydrogenations and Suzuki coupling

					
^aReduction of nitroarene					
Run	1	2	3	4	5
Yield (%)	93	92	90	89	89
					
^bReduction of C=C					
Run	1	2	3	4	5
Yield (%)	91	90	90	89	89
					
^cSuzuki coupling					
Run	1	2	3	4	5
Yield (%)	94	93	90	90	90

^aReaction conditions-nitrobenzene (0.123 g, 1 mmol), H₂, SS-PdNPs (0.2 g, 4 mol% Pd) at room temperature under aqueous medium for 0.5 h (for anilines).

^bReaction conditions: (*E*)-1-(4-chlorophenyl)-3-phenylprop-2-en-1-one (0.242 g, 1 mmol), H₂, SS-PdNPs (0.2 g, 4 mol% Pd), acetonitrile (5 mL) at room temperature for 1 h.

^cReaction conditions-4-bromoacetophenone (0.199 g, 1 mmol), benzeneboronic acid (0.145 g, 1.2 mmol), K₂CO₃ (0.207 g, 1.5 mmol), TBAB (0.154 g, 1 mmol), SS-PdNPs (0.2 g, 4 mol% Pd) and water (5 mL) at 100 °C for 0.5 h.

- performance for ethylene conversion and heptane cracking. *J. Catal.*, 289: 53-61.
- [13] Pushkarev, V.V., An, K., Alayoglu, S., Beaumont, S.K., Somorjai, G.A. (2012). Hydrogenation of benzene and toluene over size controlled Pt/SBA-15 catalysts: Elucidation of the Pt particle size effect on reaction kinetics. *J. Catal.*, 292: 64-72.
- [14] Pogorelic, I., Litvic, M.F., Merkas, S., Ljubic, G., Cepanec, I., Litvic, M. (2007). Rapid, efficient and selective reduction of aromatic nitro compounds with sodium borohydride and Raney nickel. *J. Mol. Catal. A: Chem.*, 274: 202-207.
- [15] Maity, R., Meer, M.V., Hohloch, S., Sarkar, B. (2015). Di- and Trinuclear Iridium(III) Complexes with Poly-Mesoionic Carbenes Synthesized through Selective Base-Dependent Metallation. *Organometallics*, 34: 3090-3096.
- [16] Mahdavi, H., Tamami, B. (2005). Reduction of nitro-aryl compounds with zinc in the presence of poly[N-(2-aminoethyl)acrylamido] trimethylammonium chloride as a phase-transfer catalyst. *Synth. Commun.*, 35: 1121-1127.
- [17] Smith, G.V., Nothessiz, F. (1999). *Heterogeneous Catalysis in Organic Chemistry*. Academic Press, New York.
- [18] Scheuerman, R.A., Tumelty, D. (2000). The reduction of aromatic nitro groups on solid supports using sodium hydrosulfite (Na₂S₂O₄). *Tetrahedron Lett.*, 41: 6531-6535.
- [19] Kumar, J.S.D., Ho, M.M., Toyokuni, T. (2001). Simple and chemoselective reduction of aromatic nitro compounds to aromatic amines: reduction with hydriodic acid revisited. *Tetrahedron Lett.*, 42: 5601-5604.
- [20] Mdleleni, M.M., Rinker, R., Ford, P.C. (2003). Reduction of aromatic nitro compounds as catalyzed by rhodium trichloride under water-gas shift reaction conditions. *J. Mol. Catal. A: Chem.*, 204-205: 125-131.
- [21] Chen, Y., Qiu, J., Wang, X., Xiu, J. (2006). Preparation and application of highly dispersed gold nanoparticles supported on silica for catalytic hydrogenation of aromatic nitro compounds. *J. Catal.*, 242: 227-230.
- [22] Kumbhar, P.S., Valnte, J.S., Figueras, F. (1998). Reduction of aromatic nitro compounds with hydrazine hydrate in the presence of the iron(III) oxide-MgO catalyst prepared from a MgFe hydrotalcite precursor. *Tetrahedron Lett.*, 39: 2573-2574.
- [23] Ghosh, S.K., Mandal, M., Kundu, S., Nath, S., Pal, T. (2004). Bimetallic Pt-Ni nanoparticles can catalyze reduction of aromatic nitro compounds by sodium borohydride in aqueous solution. *Appl. Catal. A: Gen.*, 268: 61-66.
- [24] Ren, P.D., Pan, S.F., Dang, T.W., Wu, H.S. (1995). The Novel Reduction Systems: NaBH₄-SbCl₃ OR NaBH₄-BiCl₃ for Conversion of Nitroarenes to Primary Amines. *Synth. Commun.*, 25: 3799-3803.
- [25] Nagaraja, D., Pasha, M.A. (1999). Reduction of aryl nitro compounds with aluminumNH₄Cl: effect of ultrasound on the rate of the reaction. *Tetrahedron Lett.*, 40: 7855-7858.
- [26] Yu, C., Liu, B., Hu, L. (2001). Samarium(0) and 1,1'-Dioctyl-4,4'-Bipyridinium Dibromide: A Novel Electron-Transfer System for the Chemoselective Reduction of Aromatic Nitro Groups. *J. Org. Chem.*, 66: 919-924.
- [27] Rylander, P.N. (1967). *Catalytic Hydrogenation over Platinum Metals*, Academic Press, New York 21.
- [28] Sterk, D., Stephan, M.S., Mohar, B. (2004). Transfer hydrogenation of activated ketones using novel chiral Ru(II)-N-arenesulfonyl-1,2-diphenylethylenediamine complexes. *Tetrahedron Lett.*, 45: 535-537.
- [29] Kaluzna, I.A., Feske, B.D., Wittayanan, W., Ghiviriga, I., Stewart, J.D. (2005). Stereoselective, Biocatalytic Reductions of α -Chloro- β -keto Esters. *J. Org. Chem.*, 70: 342-345.
- [30] Cook, P.L. (1962). Selective reduction of aldehydes to alcohols by calcined Ni-Al hydrotalcite. *J. Org. Chem.*, 27: 3873-3877.
- [31] Figadhre, B., Chaboche, C., Franck, X., Peyrat, J.F., Cave, A. (1994). Carbonyl reduction of functionalized Aldehydes and Ketone by Tri-n-butyltin Hydride and SiO₂. *J. Org. Chem.*, 59: 7138-7141.
- [32] Babler, J.H., Sarussi, S.J. (1981). Reduction of aldehydes and ketones using sodium formate in 1-methyl-2-pyrrolidinone. *J. Org. Chem.*, 46: 3367-3369.
- [33] Zhang, W., Shi, M. (2006). Reduction of activated carbonyl groups by alkylphosphines: formation of α -hydroxy esters and ketones. *Chem. Commun.*, 1218-1220.
- [34] Wang, Z.G., Wroblewski, A.E., Verkade, J.G. (1999). P(MeNCH₂CH₂)₃N: An Efficient Promoter for the Reduction of Aldehydes and Ketones with Poly(methylhydrosiloxane). *J. Org. Chem.*, 64: 8021-8023.
- [35] Sarkar, D.C., Das, A.R., Ranu, B.C. (1990). Use of zinc borohydride as an efficient and highly selective reducing agent. Selective reduction of ketones and conjugated aldehydes over conjugated enones. *J. Org. Chem.*, 55: 5799-5801.
- [36] Kim, J., De Castro, K.A., Lim, M., Rhee, H. (2010). Reduction of aromatic and aliphatic keto esters using sodium borohydride/MeOH at room temperature: a thorough investiga-

- tion. *Tetrahedron*, 66: 3995-4001.
- [37] Borch, R.F., Bernstein, M.D., Durst, H.D. (1971). Cyanohydridoborate anion as a selective reducing agent. *J. Am. Chem. Soc.*, 93: 2897-2904.
- [38] Cha, J.S., Moon, S.J., Park, J.H. (2001). A Solution of Borane in Tetrahydrofuran. A Stereoselective Reducing Agent for Reduction of Cyclic Ketones to Thermodynamically More Stable Alcohols. *J. Org. Chem.*, 66: 7514-7515.
- [39] Burkhardt, E.R., Matos, K. (2006). Boron Reagents in Process Chemistry: Excellent Tools for Selective Reductions. *Chem. Rev.*, 106: 2617-2650.
- [40] Lee, H.Y., An, M. (2003). Selective 1,4-reduction of unsaturated carbonyl compounds using $\text{Co}_2(\text{CO})_8\text{-H}_2\text{O}$. *Tetrahedron Lett.*, 44: 2775-2778.
- [41] Yu, H.T., Kang, R.H., Yang, X.M.O. (2000). Recent Development in the Selective Reduction of α,β -Unsaturated Carbonyl Compounds. *Chin. J. Org. Chem.*, 20: 441-453.
- [42] McCarthy, M., Guiry, P.J. (2001). Axially chiral bidentate ligands in asymmetric catalysis. *Tetrahedron*, 57: 3809-4058.
- [43] Hazarika, M.J., Barua, N.C. (1989). A simple procedure for selective reduction of α,β -unsaturated carbonyl compounds using Al-NiCl₂ system. *Tetrahedron Lett.*, 30: 6567-6570.
- [44] Petrier, C., Luche, J.L. (1987). Ultrasonically improved reductive properties of an aqueous ZnNiCl₂ system-1 selective reduction of α,β -unsaturated carbonyl compounds. *Tetrahedron Lett.*, 28: 2347-2350.
- [45] Alonso, F., Osante, I., Yus, M. (2006). Conjugate Reduction of α,β -Unsaturated Carbonyl Compounds Promoted by Nickel Nanoparticles. *Synlett.*, 18: 3017-3020.
- [46] Saikia, A., Barthakur, M.G., Boruah, R.C. (2005). Efficient Role of Mg-ZnCl₂ for Selective Reduction of α,β -Unsaturated Carbonyl Compounds in Aqueous Medium. *Synlett.*, 3: 523-525.
- [47] Hassan, J., Sevignon, M., Gozzi, C., Schulz, E., Lemaire, M. (2002). Aryl-Aryl Bond Formation One Century after the Discovery of the Ullmann Reaction. *Chem. Rev.*, 102: 1359-1469.
- [48] Smith, M.B., March, J. (1992). *Advanced Organic Chemistry*, 4th ed.; Wiley: New York, pp 539.
- [49] Kovacic, P., Jones, M.B. (1987). Dehydro coupling of aromatic nuclei by catalyst-oxidant systems: poly(p-phenylene). *Chem. Rev.*, 87: 357-379.
- [50] Gomberg, M., Bachmann, W.E. (1924). The synthesis of biaryl compounds by means of the diazo reaction. *J. Am. Chem. Soc.*, 42: 2339-2343.
- [51] Smith, M.B., March, J. (1992). *Advanced Organic Chemistry*, 4th ed.; Wiley: New York, pp 715.
- [52] Ullman, F., Bielecki, J. (1901). Ueber Synthesen in der Biphenylreihe. *J. Chem. Ber.*, 34: 2174-2185.
- [53] Hassan, J., Sevignon, M., Gozzi, C., Schulz, E., Lemaire, M. (2002). Aryl-Aryl Bond Formation One Century after the Discovery of the Ullmann Reaction. *Chem. Rev.*, 102: 1359-1469.
- [54] Miura, M., Nomura, M. (2002). Direct Arylation via Cleavage of Activated and Unactivated C-H Bonds. *Top. Curr. Chem.*, 219: 212-237.
- [55] Kosugi, M., Sasazawa, K., Shimizu, Y., Migita, T. (1977). Reactions of allyltin compounds iii. allylation of aromatic halides with allyltributyltin in the presence of tetrakis(triphenylphosphine)palladium(o). *Chem. Lett.*, 6: 301-302.
- [56] Kosugi, M., Shimizu, Y., Migita, T. (1977). Alkylation, arylation, and vinylation of acyl chlorides by means of organotin compounds in the presence of catalytic amounts of tetrakis(triphenylphosphine)palladium(o). *Chem. Lett.*, 6: 1423-1424.
- [57] Kosugi, M., Hagiwara, I., Migita, T. (1983). 1-Alkenylation on α -position of ketone: palladium-catalyzed reaction of tin enolates and 1-bromo-1-alkenes. *Chem. Lett.*, 12: 839-840.
- [58] Stille, J.K. (1986). The Palladium-Catalyzed Cross-Coupling Reactions of Organotin Reagents with Organic Electrophiles [New Synthetic Methods (58)]. *Angew. Chem. Int. Ed.*, 25: 508-524.
- [59] King, O., Okukado, N., Negishi, E. (1977). Highly general stereo-, regio-, and chemoselective synthesis of terminal and internal conjugated enynes by the Pd-catalysed reaction of alkynylzinc reagents with alkenyl halides. *J. Chem. Soc., Chem. Commun.*, 19: 683-684.
- [60] Lipshutz, B.H., Siegmann, K., Garcia, E., Kayser, F. (1993). Synthesis of unsymmetrical biaryls via kinetic higher order cyanocuprates: scope, limitations, and spectroscopic insights. *J. Am. Chem. Soc.*, 115: 9276-9282.
- [61] Miyaura, N., Suzuki, A. (1995). Palladium-Catalyzed Cross-Coupling Reactions of Organoboron Compounds. *Chem. Rev.*, 95: 2457-2483.

- [62] Tamao, K., Sumitani, K., Kumada, M. (1972). Selective carbon-carbon bond formation by cross-coupling of Grignard reagents with organic halides. Catalysis by nickel-phosphine complexes. *J. Am. Chem. Soc.*, 94: 4374-4376.
- [63] Corriu, R.J.P., Masse, J.P. (1972). Activation of Grignard reagents by transition-metal complexes. A new and simple synthesis of *trans*-stilbenes and polyphenyls. *J. Chem. Soc., Chem. Commun.*, 3: 144a.
- [64] Kumada, M. (1980). Nickel and palladium complex catalyzed cross-coupling reactions of organometallic reagents with organic halides. *Pure Appl. Chem.*, 52: 669-679.
- [65] Marion, N., Navarro, O., Mei, J., Stevens, E.D., Scott, N.M., Nolan, S.P. (2006). Modified (NHC)Pd(allyl)Cl (NHC = *N*-Heterocyclic Carbene) Complexes for Room-Temperature Suzuki-Miyaura and Buchwald-Hartwig Reactions. *J. Am. Chem. Soc.*, 128: 4101-4111.
- [66] Billingsley, K.L., Anderson, K.W., Buchwald, S.L. (2006). A Highly Active Catalyst for Suzuki-Miyaura Cross-Coupling Reactions of Heteroaryl Compounds. *Angew. Chem. Int. Ed.*, 45: 3484-3488.
- [67] Maity, R., Mekic, A., Meer, M.V., Verma, A., Sarkar, B. (2015). Triply cyclometalated trinuclear iridium(III) and trinuclear palladium(II) complexes with a tri-mesoionic carbene ligand. *Chem. Commun.*, 51: 15106-15109.
- [68] Majumder, A., Naskar, R., Roy, P., Maity, R. (2019). Homo- and Heterobimetallic Complexes Bearing NHC Ligands: Applications in α -Arylation of Amide, Suzuki-Miyaura Coupling Reactions, and Tandem Catalysis. *Eur. J. Inorg. Chem.*, 2019: 1810-1815.
- [69] Sodhi, R.K., Paul, S. (2015). Conversion of α,β -unsaturated ketones to 1,5-diones via tandem retro-Aldol and Michael addition using Co(acac)₂ covalently anchored onto amine functionalized silica. *Tetrahedron Lett.*, 56: 1944-1948.
- [70] Sodhi, R.K., Changotra, A., Paul, S. (2014). Metal Acetylacetonates Covalently Anchored onto Amine Functionalized Silica/Starch Composite for the One-Pot Thioetherification and Synthesis of 2H-Indazoles. *Catal Lett.*, 144:1819-1831.
- [71] Sodhi, R.K., Paul, S., Clark, J.H. (2012). A comparative study of different metal acetylacetonates covalently anchored onto amine functionalized silica: a study of the oxidation of aldehydes and alcohols to corresponding acids in water. *Green Chem.*, 14:1649-1656.
- [72] Sodhi, R.K., Paul, S. (2011). Nanosized Mn(acac)₃ Anchored on Amino Functionalized Silica for the Selective Oxidative Synthesis of 2-arylbenzimidazoles, 2-arylbenzothiazoles and Aerobic Oxidation of Benzoin in Water.

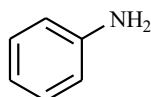
Catal Lett., 141: 608-615.

- [73] Jamwal, N., Sodhi, R.K., Gupta, P., Paul, S. (2011). Nano Pd(0) supported on cellulose: A highly efficient and recyclable heterogeneous catalyst for the Suzuki coupling and aerobic oxidation of benzyl alcohols under liquid phase catalysis. *Int. J. Biol. Macromol.*, 49: 930-935.

Appendices

Spectral data of Amines and Alcohols

Aniline (Table 2, entry 1)



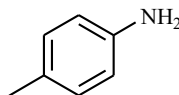
¹H NMR (CDCl₃): δ 3.72 (*bs*, 2H, NH₂), 6.74-6.76 (*d*, 2H, *J*= 8 Hz, H_{arom}), 6.85-6.88 (*t*, 1H, *J*= 6 Hz, H_{arom}), 7.24-7.28 (*t*, 1H, *J*= 8 Hz, H_{arom}).

¹³C NMR (CDCl₃): δ 115.24, 118.55, 129.40, 146.63.

IR (ν_{\max} in cm⁻¹): 3360 (NH stretch).

MS (ESI): 93 (M)⁺.

4-Toluidine (Table 2, entry 2)



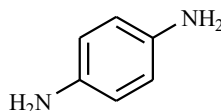
¹H NMR (CDCl₃): δ 2.30 (*s*, 3H, CH₃), 3.56 (*bs*, 2H, 2×NH₂), 6.64-6.67 (*d*, 2H, *J*= 12 Hz, H_{arom}), 7.01-7.04 (*d*, 2H, *J*= 12 Hz, H_{arom}).

¹³C NMR (CDCl₃): 20.51, 115.33, 127.83, 129.80, 143.86.

IR (ν_{\max} in cm⁻¹): 2905 (NH stretch).

MS (ESI): 107 (M)⁺.

1,4-Diamino benzene (Table 2, entry 3)



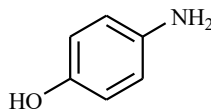
¹H NMR (CDCl₃): δ 4.01 (*bs*, 4H, NH₂), 6.25-6.30 (*m*, 4H, H_{arom}).

¹³C NMR (CDCl₃): δ 117.01, 138.22.

IR (ν_{\max} in cm⁻¹): 3010 (NH stretch).

MS (ESI): 108 (M)⁺.

4-Aminophenol (Table 2, entry 4)



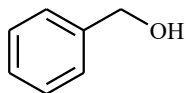
¹H NMR (CDCl₃): δ 3.92 (*bs*, 2H, NH₂), 4.95 (*s*, 1H, OH), 6.29-6.31 (*d*, 2H, *J*= 8 Hz, H_{arom}), 6.48-6.50 (*d*, 2H, *J*= 8 Hz, H_{arom}).

¹³C NMR (CDCl₃): δ 116.70, 116.82, 117.74, 140.02, 148.50.

IR (ν_{\max} in cm⁻¹): 3010 (NH stretch).

MS (ESI): 109 (M)⁺.

Benzyl alcohol (Table 2, entry 5)



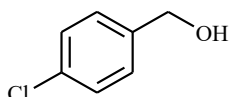
¹H NMR (CDCl₃): δ2.00 (*bs*, 1H, OH), 4.23 (*s*, 2H, CH₂), 7.19-7.23 (*m*, 5H, H_{arom}).

¹³C NMR (CDCl₃): δ65.23, 126.25, 126.27, 129.02, 140.22.

IR (ν_{max} in cm⁻¹): 3442 (O-H stretch), 2927 (CH₂ stretch).

MS (ESI): 108 (M)⁺.

4-Chlorobenzyl alcohol (Table 2, entry 6)



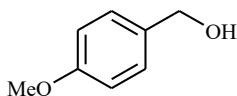
¹H NMR (CDCl₃): δ2.27 (*s*, 1H, OH), 4.64 (*s*, 2H, CH₂), 7.27-7.30 (*d*, 2H, J= 12 Hz, H_{arom}), 7.32-7.35 (*d*, 2H, J= 12 Hz, H_{arom}).

¹³C NMR (CDCl₃): δ64.46, 128.29, 128.66, 133.32, 139.25.

IR (ν_{max} in cm⁻¹): 3362 (O-H stretch), 2909 (CH₂ stretch).

MS (ESI): 142 (M)⁺, 144 (M+2).

4-Methoxybenzyl alcohol (Table 2, entry 7)



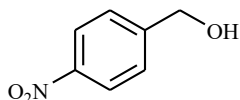
¹H NMR (CDCl₃): δ3.52 (*s*, 3H, OCH₃), 2.02 (*bs*, 1H, OH), 4.51 (*s*, 2H, CH₂), 6.70-6.72 (*d*, 2H, J= 8 Hz, H_{arom}), 7.06-7.08 (*d*, 2H, J= 8 Hz, H_{arom}).

¹³C NMR (CDCl₃): δ55.90, 68.11, 113.51, 113.63, 128.20, 133.54, 159.60.

IR (ν_{max} in cm⁻¹): 2937 (CH₂ stretch), 3390 (O-H stretch).

MS (ESI): 138 (M)⁺.

4-Nitrobenzyl alcohol (Table 2, entry 8)



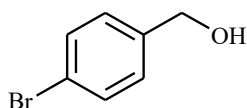
¹H NMR (CDCl₃): δ2.02 (*bs*, 1H, OH), 4.23 (*s*, 2H, CH₂), 7.45-7.48 (*d*, 2H, J= 12 Hz, H_{arom}), 8.12-8.15 (*d*, 2H, J= 12 Hz, H_{arom}).

¹³C NMR (CDCl₃): δ68.23, 121.37, 128.43, 147.66, 147.68.

IR (ν_{max} in cm⁻¹): 3508 (O-H stretch), 2926 (CH₂ stretch).

MS (ESI): 153 (M)⁺.

4-Bromobenzyl alcohol (Table 2, entry 9)



¹H NMR (CDCl₃): δ2.00 (*bs*, 1H, OH), 4.51 (*s*, 2H, CH₂), 7.08-7.10 (*d*, 2H, J= 8 Hz, H_{arom}), 7.36-7.38 (*d*,

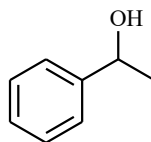
2H, J= 8 Hz, H_{arom}).

¹³C NMR (CDCl₃): δ65.20, 122.02, 129.50, 131.80, 131.92, 140.24.

IR (ν_{max} in cm⁻¹): 3357 (O-H stretch), 2915 (CH₂ stretch).

MS (ESI): 185 (M)⁺, 187 (M+2).

Phenyl ethanol (Table 2, entry 10)



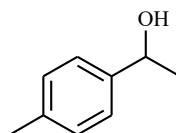
¹H NMR (CDCl₃): δ1.59 (*s*, 3H, CH₃), 2.00 (*bs*, 1H, OH), 4.17-4.23 (*q*, 1H, CH), 7.27-7.35 (*m*, 5H, H_{arom}).

¹³C NMR (CDCl₃): δ25.07, 64.46, 70.66, 128.29, 128.66, 139.25.

IR (ν_{max} in cm⁻¹): 3480 (O-H stretch), 2978 (CH stretch).

MS (ESI): 122(M)⁺.

4-Methylphenyl ethanol (Table 2, entry 11)



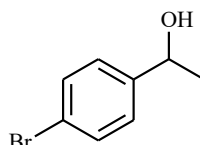
¹H NMR (CDCl₃): δ1.49 (*s*, 3H, CH₃), 2.01 (*bs*, 1H, OH), 2.35 (*s*, 3H, -CH₃), 4.64-4.70 (*q*, 1H, CH), 6.99-7.02 (*d*, 2H, J= 12 Hz, H_{arom}), 7.07-7.10 (*d*, 2H, J= 12 Hz, H_{arom}).

¹³C NMR (CDCl₃): δ22.91, 24.55, 75.73, 127.55, 137.38.

IR (ν_{max} in cm⁻¹): 3346 (O-H stretch), 2973 (CH stretch).

MS (ESI): 136(M)⁺.

4-Bromophenyl ethanol (Table 2, entry 12)



¹H NMR (CDCl₃): δ1.45 (*s*, 3H, CH₃), 1.97 (*bs*, 1H, OH), 4.41-4.45 (*q*, 1H, CH), 7.10-7.13 (*d*, 2H, J= 12 Hz, H_{arom}), 7.36-7.39 (*d*, 2H, J= 12 Hz, H_{arom}).

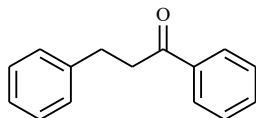
¹³C NMR (CDCl₃): δ22.54, 75.72, 121.94, 129.63, 131.92, 131.95, 140.02.

IR (ν_{max} in cm⁻¹): 3354 (O-H stretch), 2975 (CH stretch).

MS (ESI): 199(M)⁺, 201 (M+2).

Spectral data of reduced C=C double bond in α,β -unsaturated ketone^{a,b}

1,3-diphenylpropan-1-one (Table 3, entry 1)



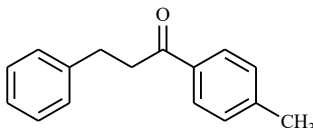
¹H NMR (CDCl₃): δ 3.06-3.09 (*t*, 2H, J= 6 Hz, CH₂), 3.30-3.33 (*t*, 2H, J= 6 Hz, CH₂), 7.18-7.96 (*m*, 10H, H_{arom}).

¹³C NMR (CDCl₃): δ 32.80, 43.92, 126.04, 127.75, 127.80, 128.92, 133.42, 136.74, 139.52, 198.22.

IR (ν_{\max} in cm⁻¹): 3062 (aromatic C-H stretch), 1682 (C=O stretch), 2922 (CH₂ stretch).

MS (ESI): 210 (M)⁺.

1-(4-Methylphenyl)-3-phenyl-propan-1-one (Table 3, entry 2)



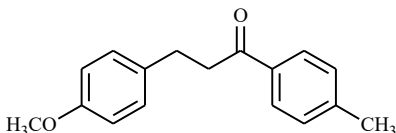
¹H NMR (CDCl₃): δ 2.32 (*s*, 3H, CH₃), 3.05-3.08 (*t*, 2H, J= 6 Hz, CH₂), 3.26-3.29 (*t*, 2H, J= 6 Hz, CH₂), 7.12-7.22 (*m*, 5H, H_{arom}), 7.35-7.37 (*d*, 2H, J= 8 Hz, H_{arom}), 7.77-7.79 (*d*, 2H, J= 8 Hz, H_{arom}).

¹³C NMR (CDCl₃): δ 24.22, 33.45, 44.01, 125.08, 127.88, 128.54, 128.77, 133.84, 139.54, 142.64, 199.05.

IR (ν_{\max} in cm⁻¹): 3058 (aromatic C-H stretch), 1681 (C=O stretch), 2921 (CH₂ stretch).

MS (ESI): 244 (M)⁺.

3-(4-Methoxyphenyl)-1-(4-methylphenyl)propan-1-one (Table 3, entry 3)



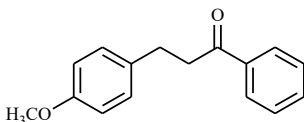
¹H NMR (CDCl₃): δ 2.42 (*s*, 3H, CH₃), 3.02-3.05 (*t*, 2H, J= 6 Hz, CH₂), 3.25-3.28 (*t*, 2H, J= 6 Hz, CH₂), 3.82 (*s*, 3H, OCH₃), 6.72-6.74 (*d*, 2H, J= 8 Hz, H_{arom}), 7.01-7.03 (*d*, 2H, J= 8 Hz, H_{arom}), 7.15-7.17 (*d*, 2H, J= 8 Hz, H_{arom}), 7.75-7.77 (*d*, 2H, J= 8 Hz, H_{arom}).

¹³C NMR (CDCl₃): δ 24.33, 32.85, 43.90, 55.92, 114.20, 128.71, 128.71, 128.85, 131.82, 133.85, 142.25, 157.22, 198.15.

IR (ν_{\max} in cm⁻¹): 3060 (aromatic C-H stretch), 1683 (C=O stretch), 2951 (CH₂ stretch).

MS (ESI): 256 (M⁺+1).

3-(4-Methoxyphenyl)-1-phenylpropan-1-one (Table 3, entry 4)



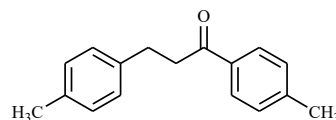
¹H NMR (CDCl₃): δ 3.03-3.06 (*t*, 2H, J= 6 Hz, CH₂), 3.25-3.28 (*t*, 2H, J= 6 Hz, CH₂), 3.80 (*s*, 3H, OCH₃), 6.83-6.85 (*d*, 2H, J= 8 Hz, H_{arom}), 7.05-7.07 (*d*, 2H, J= 8 Hz, H_{arom}), 7.75 7.98 (*m*, 5H, H_{arom}).

¹³C NMR (CDCl₃): δ 32.82, 43.90, 55.92, 114.22, 128.70, 128.82, 131.80, 133.22, 136.81, 157.91, 197.24.

IR (ν_{\max} in cm⁻¹): 3065 (aromatic C-H stretch), 1691 (C=O stretch), 2925 (CH₂ stretch).

MS (ESI): 241 (M)⁺.

1,3-(4,4'-Dimethylphenyl)propan-1-one (Table 3, entry 5)



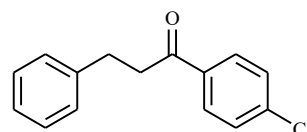
¹H NMR (CDCl₃): δ 2.34 (*s*, 3H, CH₃), 2.42 (*s*, 3H, CH₃), 3.03-3.06 (*t*, 2H, J= 6 Hz, CH₂), 3.26-3.29 (*t*, 2H, J= 6 Hz, CH₂), 7.15-7.18 (*d*, 4H, J= 12 Hz, H_{arom}), 7.82-7.85 (*d*, 4H, J= 12 Hz, H_{arom}).

¹³C NMR (CDCl₃): δ 24.33, 32.82, 43.90, 128.70, 129.02, 133.82, 135.63, 142.80, 198.22.

IR (ν_{\max} in cm⁻¹): 3059 (aromatic C-H stretch), 1685 (C=O stretch), 2919 (CH₂ stretch).

MS (ESI): 239 (M)⁺.

1-(4-Chlorophenyl)-3-phenylpropan-1-one (Table 3, entry 6)



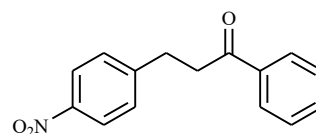
¹H NMR (CDCl₃): δ 3.12-3.15 (*t*, 2H, J= 6 Hz, CH₂), 3.37-3.40 (*t*, 2H, J= 6 Hz, CH₂), 7.08-7.78 (*m*, 7H, H_{arom}), 8.03-8.05 (*d*, 2H, J= 8 Hz, H_{arom}).

¹³C NMR (CDCl₃): δ 32.45, 44.02, 125.22, 127.80, 128.75, 128.82, 134.95, 138.72, 139.55, 200.01.

IR (ν_{\max} in cm⁻¹): 3060 (aromatic C-H stretch), 1683 (C=O stretch), 2951 (CH₂ stretch).

MS (ESI): 244 (M⁺), 246 (M⁺+2).

3-(4-Nitrophenyl)-1-phenylpropan-1-one (Table 3, entry 7)



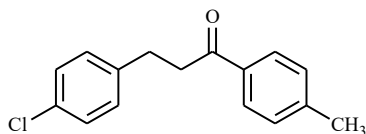
¹H NMR (CDCl₃): δ 3.40-3.43 (*t*, 2H, J= 6 Hz, CH₂), 3.70-3.73 (*t*, 2H, J= 6 Hz, -CH₂), 7.23-7.85 (*m*, 5H, H_{arom}), 7.90-7.92 (*d*, 2H, J= 8 Hz, H_{arom}), 8.28-8.30 (*d*, 2H, J= 8 Hz, H_{arom}).

¹³C NMR (CDCl₃): δ 31.89, 45.05, 121.02, 128.77, 128.89, 133.25, 136.84, 145.62, 198.05.

IR (ν_{\max} in cm⁻¹): 3013 (aromatic C-H stretch), 1675 (C=O stretch), 2963 (CH₂ stretch).

MS (ESI): 255 (M⁺).

3-(4-Chlorophenyl)-1-(4-methylphenyl) propan-1-one (Table 3, entry 8)



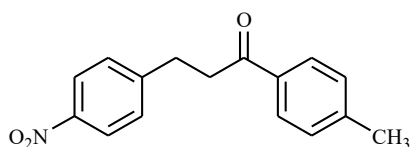
$^1\text{H NMR}$ (CDCl_3): δ 2.35 (s, 3H, CH_3), 3.04-3.08 (t, 2H, $J=8$ Hz, CH_2), 3.24-3.28 (t, 2H, $J=8$ Hz, CH_2), 7.21-7.33 (m, 4H, H_{arom}), 7.84-7.87 (d, 2H, $J=12$ Hz, H_{arom}), 7.93-7.96 (d, 2H, $J=12$ Hz, H_{arom}).

$^{13}\text{C NMR}$ (CDCl_3): δ 24.30, 32.84, 43.90, 128.72, 128.84, 129.05, 129.22, 130.54, 137.64, 142.22, 200.02

IR (ν_{max} in cm^{-1}): 3056 (aromatic C-H stretch), 1682 (C=O stretch), 2942 (CH_2 stretch).

MS (ESI): 258 (M^+), 260 (M^{++}).

3-(4-Nitrophenyl)-1-(4-methylphenyl) propan-1-one (Table 3, entry 9)



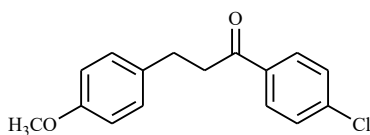
$^1\text{H NMR}$ (CDCl_3): δ 3.03-3.07 (t, 2H, $J=8$ Hz, CH_2), 3.28-3.32 (t, 2H, $J=8$ Hz, CH_2), 7.18-7.20 (d, 2H, $J=8$ Hz, H_{arom}), 7.26-7.28 (d, 2H, $J=8$ Hz, H_{arom}), 7.56-7.58 (d, 2H, $J=8$ Hz, H_{arom}), 7.94-7.96 (d, 2H, $J=8$ Hz, H_{arom}).

$^{13}\text{C NMR}$ (CDCl_3): δ 26.66, 32.80, 43.90, 127.23, 127.25, 127.68, 128.95, 135.72, 139.80, 145.87, 198.24.

IR (ν_{max} in cm^{-1}): 3032 (aromatic C-H stretch), 1679 (C=O stretch), 2945 (CH_2 stretch).

MS (ESI): 270 (M^+).

1-(4-Chlorophenyl)-3-(4-methoxyphenyl) propan-1-one (Table 3, entry 10)



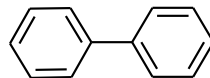
$^1\text{H NMR}$ (CDCl_3): δ 3.04-3.07 (t, 2H, $J=6$ Hz, CH_2), 3.28-3.31 (t, 2H, $J=6$ Hz, CH_2), 3.98 (s, 3H, OCH_3), 6.95-6.98 (d, 2H, $J=12$ Hz, H_{arom}), 7.25-7.68 (m, 4H, H_{arom}), 7.97-8.0 (d, 2H, $J=12$ Hz, H_{arom}).

$^{13}\text{C NMR}$ (CDCl_3): δ 24.30, 32.84, 43.90, 121.92, 128.71, 128.73, 133.84, 142.88, 145.02, 146.66, 199.05.

IR (ν_{max} in cm^{-1}): 3003 (aromatic C-H stretch), 1677 (C=O stretch), 2964 (CH_2 stretch). MS (ESI): 275 (M^+).

Spectral data of Cross coupling Suzuki reaction

Biphenyl (Table 2, entry 1)



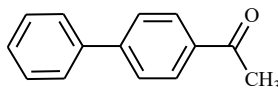
$^1\text{H NMR}$ (CDCl_3): δ 7.48-7.74 (m, 10H, H_{arom}).

$^{13}\text{C NMR}$ (CDCl_3): δ 127.74, 127.92, 129.33, 136.58.

IR (ν_{max} in cm^{-1}): 3105 (aromatic C-H stretch).

MS (ESI): 154 (M^+).

4-Acetylbiphenyl (Table 2, entry 2)



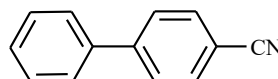
$^1\text{H NMR}$ (CDCl_3): δ 2.64 (s, 3H, COCH_3), 7.40-7.49 (m, 5H, H_{arom}), 7.61-7.63 (d, 2H, $J=8$ Hz, H_{arom}), 7.67-7.69 (d, 2H, $J=8$ Hz, H_{arom}).

$^{13}\text{C NMR}$ (CDCl_3): δ 26.66, 127.23, 127.25, 128.26, 128.94, 128.95, 135.72, 139.80, 145.87, 198.24.

IR (ν_{max} in cm^{-1}): 3040 (aromatic C-H stretch), 2920 (C-H stretch), 1690 (C=O stretch).

MS (ESI): 196 (M^+).

4-Phenylbenzonitrile (Table 2, entry 3)



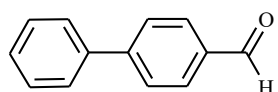
$^1\text{H NMR}$ (CDCl_3): δ 7.43-7.53 (m, 3H, H_{arom}), 7.60-7.63 (d, 2H, $J=12$ Hz, H_{arom}), 7.69-7.71 (d, 2H, $J=8$ Hz, H_{arom}), 7.74-7.76 (d, 2H, $J=8$ Hz, H_{arom}).

$^{13}\text{C NMR}$ (CDCl_3): δ 110.89, 118.99, 127.25, 127.75, 128.15, 128.69, 128.97, 129.14, 132.62, 132.91, 139.18, 145.69.

IR (ν_{max} in cm^{-1}): 3051 (aromatic C-H stretch), 2235 (CN stretch).

MS (ESI): 179 (M^+).

Biphenyl-4-carboxaldehyde (Table 2, entry 4)



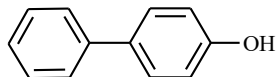
$^1\text{H NMR}$ (CDCl_3): δ 7.40-7.71 (m, 5H, H_{arom}), 7.75-7.77 (d, 1H, $J=8$ Hz, H_{arom}), 7.95-7.97 (d, 1H, $J=8$ Hz, H_{arom}), 8.17-8.19 (d, 2H, $J=8$ Hz, H_{arom}), 10.02 (s, 1H, -CHO).

$^{13}\text{C NMR}$ (CDCl_3): δ 127.70, 127.95, 128.47, 129.32, 130.46, 136.22, 142.35, 191.50.

IR (ν_{max} in cm^{-1}): 3042 (aromatic C-H stretch), 2922 (C-H stretch), 1688 (C=O stretch).

MS (ESI): 183 (M^+).

4-Phenylphenol (Table 2, entry 5)



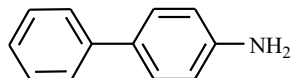
$^1\text{H NMR}$ (CDCl_3): δ 5.01 (s, 1H, -OH), 6.85-6.87 (d, 2H, $J=8$ Hz, H_{arom}), 7.38-7.55 (m, 7H, H_{arom}).

$^{13}\text{C NMR}$ (CDCl_3): δ 116.40, 127.77, 127.90, 129.18, 129.33, 136.55, 157.44.

IR (ν_{max} in cm^{-1}): 3597 (O-H stretch), 3045 (aromatic C-H stretch).

MS (ESI): 170 (M) $^+$.

4-Phenylphenylamine (Table 2, entry 6)



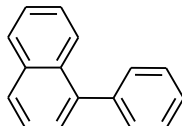
$^1\text{H NMR}$ (CDCl_3): δ 4.95 (bs, 2H, -NH $_2$), 6.88-6.90 (d, 2H, $J=8$ Hz, H_{arom}), 7.45-7.68 (m, 7H, H_{arom}).

$^{13}\text{C NMR}$ (CDCl_3): δ 116.80, 126.54, 127.73, 127.92, 128.55, 128.76, 136.56, 147.28.

IR (ν_{max} in cm^{-1}): 3200 (N-H stretch), 3042 (aromatic C-H stretch).

MS (ESI): 169 (M) $^+$.

1-Phenyl-naphthalene (Table 2, entry 7)



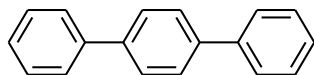
$^1\text{H NMR}$ (CDCl_3): δ 7.30-7.77 (m, 14H, H_{arom}).

$^{13}\text{C NMR}$ (CDCl_3): δ 125.22, 126.36, 126.36, 126.81, 127.71, 127.92, 129.33, 129.42, 133.15, 133.54, 136.54, 136.72.

IR (ν_{max} in cm^{-1}): 3055 (aromatic C-H stretch).

MS (ESI): 205 (M) $^+$.

4-(Phenyl) biphenyl (Table 2, entry 8)



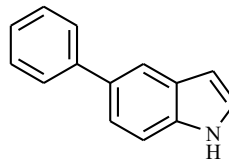
$^1\text{H NMR}$ (CDCl_3): δ 7.45-7.46 (m, 4H, H_{arom}), 7.70-7.72 (m, 4H, H_{arom}), 8.01-8.03 (m, 4H, H_{arom}).

$^{13}\text{C NMR}$ (CDCl_3): δ 122.07, 126.17, 126.38, 126.80, 129.08, 135.61, 140.20, 141.08.

IR (ν_{max} in cm^{-1}): 3050 (aromatic C-H stretch).

MS (ESI): 230 (M) $^+$.

5-Phenyl-1-H-indole (Table 2, entry 9)



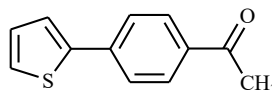
$^1\text{H NMR}$ (CDCl_3): δ 6.61-6.64 (d, 1H, $J=12$ Hz, H_{arom}), 7.23-7.24 (m, 1H, H_{arom}), 7.41-7.45 (m, 5H, H_{arom}), 7.66-7.69 (d, 2H, $J=12$ Hz, H_{arom}), 7.86-7.89 (d, 1H, $J=12$ Hz, H_{arom}), 8.15 (bs, 1H, NH).

$^{13}\text{C NMR}$ (CDCl_3): δ 102.40, 111.62, 117.05, 124.33, 127.72, 127.91, 129.30, 134.45, 136.54, 143.71.

IR (ν_{max} in cm^{-1}): 3250 (N-H stretch), 3048 (aromatic C-H stretch).

MS (ESI): 195 (M) $^+$.

2-(4-Acetylphenyl)thiophene (Table 2, entry 10)



$^1\text{H NMR}$ (CDCl_3): δ 2.61 (s, 3H, COCH $_3$), 7.02-7.08 (t, 2H, $J=12$ Hz, H_{arom}), 7.20-7.23 (d, 1H, $J=12$ Hz, H_{arom}), 7.36-7.39 (d, 1H, $J=12$ Hz, H_{arom}), 7.52-7.55 (d, 2H, $J=12$ Hz, H_{arom}), 7.90-7.93 (d, 2H, $J=12$ Hz, H_{arom}).

$^{13}\text{C NMR}$ (CDCl_3): δ 29.36, 128.01, 128.59, 128.65, 129.84, 131.85, 133.20, 136.71, 139.73, 198.90.

IR (ν_{max} in cm^{-1}): 3051 (aromatic C-H stretch), 2801 (C-H stretch), 1720 (C=O stretch), 1582 (C-S stretch).

MS (ESI): 203 (M) $^+$.